



Impact of Amylose-Amylopectin Ratio of Starches on the Mechanical Strength and Stability of Acetylsalicylic Acid Tablets

Natalia Veronica¹ · Celine Valeria Liew² · Paul Wan Sia Heng¹

Received: 22 December 2021 / Accepted: 23 March 2022 / Published online: 20 April 2022
© The Author(s) 2022

Abstract

The two main components of starch — amylose and amylopectin, are responsible for its interaction with moisture. This study investigated how moisture sorption properties of the starches with different amylose-amylopectin ratio impacted tablet properties including drug stability. The starch samples were equilibrated to 33, 53, and 75% relative humidity (RH) and then assessed for tableability, compactibility, and yield pressure. Effect of humidity on viscoelastic recovery was also evaluated. Tableability and compactibility of high-amylose starch were better than that of high-amylopectin starch at 33 and 53% RH. However, at 75% RH, the reverse was observed. In terms of yield pressure, high-amylose starch had lower yield pressure than high-amylopectin starch. High-amylose starch tablets also exhibited lower extent of viscoelastic recovery than high-amylopectin starch tablets. The variations in the tableting properties were found to be related to relative locality of the sorbed moisture. Degradation of acetylsalicylic acid in high-amylose starch tablets at 75% RH, 40°C was less than the tablets with high-amylopectin starch. This observation could be attributed to the greater amount of water molecules binding sites in high-amylose starch. Furthermore, most of the sorbed moisture of high-amylose starch was internally absorbed moisture, therefore limiting the availability of diffusible sorbed moisture for degradation reaction. Findings from this study could provide better insights on the influence of amylose-amylopectin ratio on tableting properties and stability of moisture-sensitive drugs. This is of particular importance as starch is a common excipient in solid dosage forms.

Keywords Amylopectin · Amylose · Moisture · Stability · Tableting

INTRODUCTION

The interaction between water and solids is of paramount importance in the formulation, processing, and product performance of pharmaceutical solid dosage forms. Exposure of materials to moisture is known to influence flow, tableability, drug stability, and dissolubility (1–9). Due to the ubiquitous nature of moisture, it is not possible or desirable to completely remove moisture as moisture is necessary for

bond formation and manufacturing processes often involve water. However, moisture exposure can be kept short and residual moisture level low in the products while post-manufacture products can be protected by coating or packaging such that deleterious effects of moisture may be minimized.

Water can associate with solids in two ways — adsorption and absorption (10). Interaction of water at the surface as a monolayer (primary layer of water molecules tightly bound on available surface of solids) and as multilayer moisture (moisture layer that is formed beyond the monolayer as more water molecules adsorbed on the monolayer moisture) is termed as adsorption. Penetration of water into the bulk solid structure is known as absorption. The term sorption is commonly used to describe a state when both adsorption and absorption occur. The sorbed moisture can be further classified into bound and unbound moisture (11–13). Additionally, moisture can also be grouped based on relative distribution in solids as (1) monolayer moisture, (2) externally adsorbed moisture condensed on the monolayer, and (3) bound moisture as internally absorbed moisture (14, 15). The extent

✉ Celine Valeria Liew
celine.liew@monash.edu

✉ Paul Wan Sia Heng
phapaulh@nus.edu.sg

¹ Department of Pharmacy, GEA-NUS Pharmaceutical Processing Research Laboratory, National University of Singapore, 18 Science Drive 4, Singapore 117543, Singapore

² School of Pharmacy, Monash University Malaysia, Jalan Lagoon Selatan, 47500 Subang Jaya, Selangor, Malaysia

of multilayer moisture can be approximated by subtracting monolayer moisture from externally adsorbed moisture (1). Availability of the sorbed moisture for a reaction, however, may not be similar across different materials. Water activity is a unitless parameter that ranges from 0 to 1 and can be derived from the ratio of water vapor partial pressure divided by saturation pressure. Water activity reflects the escaping tendency or fugacity of water from a substrate. Accordingly, water activity gives an indication of the degree freely available moisture for reaction and hence, the reactivity (16).

The solid-moisture interactions depend largely on the physicochemical properties of the materials. Nokhodchi *et al.* (1) reported an increase in moisture uptake with increasing particle size of hydroxypropyl methylcellulose. Similarly, Agrawal *et al.* (17) observed differences in distribution of sorbed moisture in relation to the particle size of ethylcellulose whereby larger particles had more internally absorbed moisture and less externally adsorbed moisture. However, Saripella *et al.* (18) reported no significant effect of crospovidone particle size on moisture affinity of the material and that similar moisture distribution patterns were observed. Besides particle size, molecular arrangements in solids (crystalline or amorphous structure) can also determine their interaction with moisture (19, 20). Mihranyan *et al.* (20) suggested that structural properties of the materials including surface area and pore volume should be considered along with crystallinity, when evaluating moisture interactions. Particle porosity was also found to affect the state of moisture found in the material, as bound or unbound moisture (21). Yet, another study showed similar moisture uptake when the particle porosity was varied (22). Therefore, various physicochemical properties of the materials have to be examined holistically to explain moisture-solid interactions.

Starch is a natural carbohydrate polymer comprising of two main polysaccharides, amylose and amylopectin, and some minor secondary components (proteins, lipids, and minerals) in relatively small fractions (23). Depending on the botanical origins, the starches differ slightly in their compositions. Amylose-amylopectin ratio has been reported to influence gelatinization temperature, gelling/pasting behavior, swelling, crystallinity, and moisture interaction of starches (24–26). Starch can also be modified to confer suitable properties for specific purposes. The modifications of starch including but not limited to etherification, esterification, crosslinking, oxidation, cationization, and grafting could potentially alter properties of starch (27–29). However, modification may alter moisture interactivity of the starch.

In the pharmaceutical industry, starch is commonly used as a multifunctional excipient, functioning as a binder, disintegrant, diluent, or glidant (30). Different starches have been evaluated for their performance as tablet diluent. Differences

in terms of the compression behavior of starches were attributed to variations not only in constituents but also in physical attributes such as shape, size, and size distribution. Paronen and Juslin (31) reported that particle rearrangement had minimal effect on the densification of larger starch granules (e.g., potato starch) during compression. On the contrary, the densification of smaller starch granules (e.g., maize starch) was primarily due to particle rearrangement. It has also been reported that gelling property of amylose contributes to formation of tablets having higher tensile strength (32). Starches of different botanical origins also exhibited differences in distribution of sorbed moisture and notably, a tablet formulation that contains starch with more of the moisture held as internally absorbed moisture had lower drug degradation (33).

Despite the massive amount of information on the structure and composition of starch, there is still limited literature information on moisture effects relating to tableting and drug stability of starch-based formulations. Also, variations of starch grains in their shape, size, and size distribution could confound the findings related to the differences in amylose-amylopectin ratio. Accordingly, it is essential to obviate variations due to physical attributes. Therefore, the aim of this investigation was to unravel the moisture properties of starches having different amylose-amylopectin ratio and to relate the findings to tableting properties and drug stability. Interaction of starch with moisture can be of consequential interest in formulations containing moisture-sensitive drugs or components. In the study, moisture interaction of the starches was evaluated by the moisture sorption-desorption isotherm and distribution pattern of the sorbed moisture. Effects of moisture on tableting properties, including tableting ability, compactibility, and yield pressure, were investigated. Viscoelastic recovery of the tablets was also assessed. Lastly, stability of moisture-sensitive drugs in tablets formulated with starch was evaluated at 75% RH, 40°C.

MATERIALS AND METHODS

Materials

Native maize starches of different amylose-amylopectin ratio were used: high-amylose maize starch (amylose \geq 88%; maize starch amylo N-400, Roquette, France) and high-amylopectin maize starch (amylopectin \geq 88%; waxy maize starch N-200, Roquette, France) (34, 35). Acetylsalicylic acid (ASA; USP grade, Bengbu Bayi Pharmaceuticals, China) was used as the model drug. The presence of ester functional group makes ASA susceptible to degradation by hydrolysis.

Magnesium chloride hexahydrate ($\text{MgCl}_2 \cdot 6\text{H}_2\text{O}$; Merck Chemicals, Germany), magnesium nitrate hexahydrate

($\text{Mg}(\text{NO}_3)_2 \cdot 6\text{H}_2\text{O}$; Merck Chemicals, Germany), and sodium chloride (NaCl; Merck Chemicals, Germany) were used for maintaining RH conditions of 33, 53, and 75% RH, respectively (36). For evaluation of ASA degradation, the following solvents were used — acetonitrile (HPLC Grade, Fisher Chemical, USA), ortho-phosphoric acid (Merck Chemicals, Germany), and purified water.

Conditioning of Starch

Prior to RH conditioning, the starch samples were oven-dried at 60°C for at least 12 h. Subsequently, the oven-dried samples were stored at 25°C for at least 2 weeks over a series of saturated inorganic salt slurries of $\text{MgCl}_2 \cdot 6\text{H}_2\text{O}$, $\text{Mg}(\text{NO}_3)_2 \cdot 6\text{H}_2\text{O}$, and NaCl for storage conditions of 33, 53, and 75% RH, respectively.

Assessment of Morphology

Morphology of the starch was examined under a scanning electron microscope (SEM; JSM-6010LV, JEOL, Japan). The starch sample was mounted on a sample holder using a copper tape and subjected to sputter coating with platinum (MSP-2S, IXRF Systems, USA) prior to observation at 500× magnification with 2.5-kV accelerating voltage.

Characterization of Starch Grain Size

Images of at least 600 grains were randomly captured using a SEM (JSM-6010LV, JEOL, Japan). Size of the grains was measured with the in-built software (InTouchScope, JSM-6010, v.1.11). Size characterization was performed in terms of D_{10} , D_{50} , and D_{90} , which correspond to the 10th, 50th, and 90th percentile grain sizes, respectively. The size distribution was calculated as span based on Eq. 1.

$$\text{Span} = \frac{D_{90} - D_{10}}{D_{50}} \quad (1)$$

Powder X-ray Diffraction

Structure of the starch was characterized for X-ray diffraction pattern (XRD; XRD-6000, Shimadzu, Japan). The XRD pattern was evaluated for starch samples that had been conditioned to 33, 53, and 75% RH. The sample was scanned (Cu-K α radiation source, 40 kV, 30 mA) from 5 to 50° 2 θ , in 0.02° steps at 2°/min. Relative crystallinity of the sample was estimated using the software (XRD-6100/7000 v.7.00), based on the ratio between crystalline peaks and total intensity. The determination of relative crystallinity was performed in triplicates and averaged results reported.

Evaluation of Starch Interaction with Moisture

Moisture Content

Moisture contents of the oven-dried and RH equilibrated starch were measured by drying approximately 500 mg of the sample at 105°C (HE73, Mettler Toledo, Switzerland) until a constant sample weight. The moisture content was subsequently calculated based on Eq. 2.

$$\text{Moisture content}(\%) = \frac{[\text{initial weight}] - [\text{final weight}]}{[\text{initial weight}]} \times 100 \quad (2)$$

Dynamic Moisture Sorption-Desorption Isotherm

The moisture sorption-desorption isotherm was obtained using a vapor sorption analyzer (Aqualab, Meter Group, USA) at 25°C. Approximately 1000 mg of oven-dried starch sample was placed in the sample chamber and subjected to conditions of increasing RH from 10 to 90% (sorption process) and decreasing RH of 90 to 10% (desorption process). The starch sample was equilibrated to each RH condition before moving to the next RH conditions. Equilibration was achieved when change in the sample mass with time was less than 0.05%/h.

Data from the sorption-desorption isotherm was fitted using a non-linear regression analysis to the Guggenheim-Anderson-de Boer (GAB) model (Eq. 3).

$$M_w = \frac{M_m C_{GAB} K_{GAB} a_w}{(1 - K_{GAB} a_w)(1 - K_{GAB} a_w + C_{GAB} K_{GAB} a_w)} \quad (3)$$

where M_w is the equilibrium moisture content, M_m is the monolayer moisture content, C_{GAB} is a constant that represents total heat of the first layer of sorption, and K_{GAB} is a constant that is related to multilayer sorption. a_w refers to water activity. Specific surface area (SSA) was derived from M_m using Eq. 4.

$$\text{SSA} = \frac{M_m N A_w}{W_w} \quad (4)$$

where N , A_w , and W_w refer to Avogadro's number ($6.02 \times 10^{23} \text{ mol}^{-1}$), area covered by one water molecule ($10.60 \times 10^{-20} \text{ m}^2$), and the molecular weight of water (18.02 g/mol), respectively.

Area of hysteresis loop was obtained by taking the difference between area under curve (AUC) of the sorption and desorption isotherms (Eq. 5).

$$\text{Area of hysteresis loop} = \text{AUC}_{\text{desorption}} - \text{AUC}_{\text{sorption}} \quad (5)$$

Locality of Sorbed Moisture

Data from the moisture sorption isotherm was also fitted into the Young and Nelson model to evaluate locality of sorbed moisture (Eqs. 6–13) (14, 15).

$$\theta_{Y-N} = \frac{RH}{RH + (1 - RH)E} \quad (6)$$

where θ_{Y-N} is the fraction of surface covered by a monolayer of water molecules. RH is the relative humidity and E is a constant unique to each material, which can be expressed by Eq. 7.

$$E = \exp \frac{-(q_l - q_s)}{k_B T} \quad (7)$$

where q_l is the heat of adsorption of water molecules on the surface, q_s is the normal heat of condensation of water molecules (40.8 kJ/mol), k_B is the Boltzmann's constant (1.38×10^{-23} J/K), and T is the absolute temperature.

To calculate the fraction of surface covered by multilayer moisture (Φ), Eq. 8 was used. Equation 9 was used to determine total amount of adsorbed moisture in the multilayer (α).

$$\Phi = (RH)\theta_{Y-N} \quad (8)$$

$$\alpha = -\frac{E(RH)}{E - (E - 1)RH} + \frac{E^2}{E - 1} \ln \frac{E - (E - 1)RH}{E} - (E + 1) \ln(1 - RH) \quad (9)$$

From θ_{Y-N} , Φ , and α , locality of moisture as monolayer ($A_{Y-N}\theta_{Y-N}$), externally adsorbed moisture ($A_{Y-N}(\theta_{Y-N} + \alpha)$), and internally absorbed moisture ($B_{Y-N}\Phi$) were obtained from Eqs. 10 and 11.

$$M_s = A_{Y-N}(\theta_{Y-N} + \alpha) + B_{Y-N}\Phi \quad (10)$$

$$M_d = A_{Y-N}(\theta_{Y-N} + \alpha) + B_{Y-N}\theta_{Y-N}RH_{max} \quad (11)$$

where M_s and M_d refer to moisture contents of the sample during the sorption and desorption phases, respectively. RH_{max} is the maximum relative humidity. A_{Y-N} and B_{Y-N} are constants unique to each material and can be expressed using Eqs. 12 and 13, respectively.

$$A_{Y-N} = \frac{\rho_w V_m}{W_w} \quad (12)$$

$$B_{Y-N} = \frac{\rho_w V_a}{W_m} \quad (13)$$

where ρ_w is the water density (1 g/mL). W_m refers to the dry sample weight used, which was 1000 mg. V_m and V_a

are the volumes of the adsorbed and absorbed moisture, respectively.

As multilayer moisture is contributed by monolayer ($A_{Y-N}\theta_{Y-N}$) and externally adsorbed moisture ($A_{Y-N}(\theta_{Y-N} + \alpha)$), multilayer moisture can be estimated from Eq. 14 (1).

$$\text{Multilayer moisture} = A_{Y-N}(\theta_{Y-N} + \alpha) - (A_{Y-N}\theta_{Y-N}) \quad (14)$$

Characterization of Tableting Properties

Evaluation of Tableability and Compactibility

Compression was performed on starch samples that had been equilibrated to different RH conditions (33, 53, and 75% RH). Starch, 200 mg per tablet, was compressed into tablets at different pressures — 64, 127, 191, 255, and 318 MPa using a compaction simulator (STYL'One Evolution, Medel-Pharm, France). Flat face punches and die set of 10-mm diameter (Natoli Engineering Company, USA) were used for the compression. The upper and lower punches were set to move at a linear speed of 35 mm/s. Only freshly withdrawn samples of RH conditioned starch were used for compression into tablets. Immediately after preparation, the tablets were kept in the corresponding RH chamber at 25°C until required for analysis. Tablet evaluation was carried out on tablets that have been kept for at least 24 h post-production.

Tableability describes tablet tensile strength as a function of applied compression pressure. Tableability profile was obtained by plotting a graph of tablet tensile strength against the compression pressure. Slope of the linear line of the plot was used as a tableability index.

Tablet tensile strength (σ) was calculated according to Eq. 15. The tensile strength was determined using five randomly chosen tablets and results were averaged.

$$\sigma = \frac{2F}{\pi D_{24h} H_{24h}} \quad (15)$$

where F refers to the tablet breaking force and was measured using a hardness tester (TBF 1000, Copley Scientific, UK). Thickness of tablet was measured 24 h after production (H_{24h}) using a thickness gauge (Mitutoyo Absolute, 547-300S, Japan). The same thickness gauge was also used to obtain the tablet diameter (D_{24h}).

Compactibility is the ability of a material to form a compact of sufficient strength. The compactibility of a material can be evaluated from a plot of tablet tensile strength against tablet porosity at different compression pressures. Tablet porosity (ϵ) was calculated based on Eq. 16.

$$\epsilon = 1 - \frac{\rho_{app}}{\rho_{true}} \quad (16)$$

where ρ_{app} and ρ_{true} refer to the apparent density and true density of the material, respectively. ρ_{app} was calculated using Eq. 17. ρ_{true} was measured using a helium pycnometer (Pentapycnometer, Quantachrome Instruments, USA). ρ_{true} was measured on dried starch to minimize influence of volatile moisture on the measurement.

$$\rho_{app} = \frac{W}{\pi r_{24h}^2 H_{24h}} \quad (17)$$

where W is the tablet weight. The tablet was weighed using an analytical weighing balance with a readability up to 0.1 mg and reproducibility of ± 0.1 mg (QUINTIX224-1CEU, Sartorius Lab Instruments GmbH & Co. KG, Germany). r_{24h} is the tablet radius measured 24 h post-production. r_{24h} was derived from the tablet diameter, which was measured using a thickness gauge.

The Ryshkewitch-Duckworth equation (Eq. 18) can be transformed into a linear equation. By plotting \ln tensile strength against tablet porosity, information on tablet tensile strength at zero porosity (σ_0) and constant b , which is related to pore distribution within a tablet, can be obtained (37, 38).

$$\sigma = \sigma_0 e^{-be} \quad (18)$$

Determination of Yield Pressure

Yield pressure of the starch sample was indirectly determined by assessing compressibility of the sample. Compressibility refers to the ability of a material to undergo volume reduction. For the assessment of compressibility, 500 mg of starch was compressed using a compaction simulator (STYL'One Evolution, MedelPharm, France) installed with 14-mm flat face punches and die set (Natoli Engineering Company, USA). The upper and lower punches were set to move at 15 mm/min linear compression speed to achieve maximum compression pressure of 95 MPa. Changes in the tablet thickness with compression pressure were recorded and used in computation of the ρ_{app} using the Analis software (AnalisMX v2.07.08).

Heckel equation (Eq. 19) (39) was used to analyze the compressibility, based on in-die method.

$$\ln \left[\frac{1}{(1-D)} \right] = K_H P + A_H \quad (19)$$

where K_H and A_H are obtained from the slope and y -intercept of the linear portion of the Heckel plot, respectively. K_H is a constant related to ability of a material to undergo plastic deformation. The reciprocal of K_H is equivalent to yield pressure, which indicates compressibility of the material. A_H is a constant related to degree of packing that can be achieved by particle rearrangement

before considerable interparticle bonding takes place. D is the relative density, obtained from the ratio between ρ_{app} and ρ_{true} at compression pressure, P .

The extent of particle rearrangement in the die was further evaluated in terms of D_a (relative density during the initial densification resulting from die filling, particle slippage, and rearrangement), D_0 (relative density at zero applied pressure), and D_b (relative density due to the change in density resulting from particle rearrangement). From the value of A_H obtained from the y -intercept of the linear portion of the Heckel plot, D_a was calculated using the following equations (Eqs. 20 and 21).

$$A_H = \ln \left[\frac{1}{(1-D_a)} \right] \quad (20)$$

$$D_a = 1 - e^{-A_H} \quad (21)$$

Similarly, using 0_H obtained from the starting point of the Heckel plot before compression starts, D_0 was calculated according to Eqs. 22 and 23.

$$0_H = \ln \left[\frac{1}{(1-D_0)} \right] \quad (22)$$

$$D_0 = 1 - e^{-0_H} \quad (23)$$

D_b was obtained by taking the difference between D_a and D_0 (Eq. 24).

$$D_b = D_a - D_0 \quad (24)$$

Evaluation of Viscoelastic Recovery

Tablets for the evaluation of viscoelastic recovery were produced in the same manner as described in the section on evaluation of tabletability and compactibility. To account for changes in the axial and radial directions, the viscoelastic recovery was assessed by measuring tablet dimensions (height and diameter) using a thickness gauge. Tablet dimensions were measured immediately and 24 h after production to obtain tablet volume immediately (V_{imm}) (Eq. 25) and 24 h post-production (V_{24h}) (Eq. 26).

$$V_{imm} = \pi \times r_{imm}^2 \times H_{imm} \quad (25)$$

$$V_{24h} = \pi \times r_{24h}^2 \times H_{24h} \quad (26)$$

where r_{imm} and H_{imm} refer to the tablet radius and thickness measured immediately after production.

The viscoelastic recovery was then expressed as change in tablet dimensions according to Eq. 27.

$$\text{Change in tablet dimensions (\%)} = \frac{V_{24h} - V_{imm}}{V_{24h}} \times 100 \quad (27)$$

Degradation of ASA

Tablet Preparation

Tablets, each weighing 300 mg, comprising starch and ASA (4:1, w/w) were produced using a compaction simulator (STYL'One Evolution, MedelPharm, France). Prior to tablet production, powder mixture was prepared by mixing starch and ASA in a glass bottle (diameter: 5.5 cm, height: 5.5 cm) with a figure of 8 mixing motion for 3 min. An accurately weigh amount of powder mixture was then filled manually into the die. The compression was performed using 10-mm flat face punches and die set (Natoli Engineering Company, USA) with both the upper punch and lower punch linear compression speeds set at 35 mm/s. Compression pressure of 191 MPa was used. Three batches of tablets were produced, with the starch fractions as (A) high-amylose starch, (B) mixture of high-amylose and high-amylopectin starches in 1:1 ratio, and (C) high-amylopectin starch. The tablets immediately after fabrication were stored under 75% RH, 40°C to accelerate ASA degradation. The tablets were also evaluated for viscoelastic recovery. The evaluation was performed on five randomly chosen tablets according to the method described in the previous section.

Evaluation of ASA Degradation

Tablets containing ASA were evaluated for ASA degradation using a HPLC method as previously reported (33). The tablets were evaluated 7, 14, 28, 60, and 90 days after production. At each sampling time point, at least three randomly chosen tablets were evaluated for ASA degradation and results were averaged. Individual tablet was pulverized in a mortar using a pestle. Subsequently, about 150 mg of the pulverized powder, accurately weighed, was mixed with a menstruum of acetonitrile:water (35:65, v/v) to 10 mL and ultrasonicated (LC60H, Elma, Germany) for a minute before passing through a 0.45- μm filter (regenerated cellulose; Sartorius, Germany) prior to HPLC analysis. The filtrate (20 μL) was next injected into the HPLC column for analysis. A reversed phase C-18 column (ACE Generix, 5 μm , 4.6 mm \times 100 mm, Advanced Chromatography Technologies, UK) was used as the stationary phase and maintained at 40°C. The mobile phase comprising acetonitrile:water:ortho-phosphoric acid (35:65:0.2, v/v/v) was eluted at 0.8 mL/min using an

isocratic elution mode. Detection of ASA and its degradant, salicylic acid (SA), was carried out at 273 and 296 nm for ASA and SA, respectively. The percentage degradation of ASA was calculated using Eq. 28.

$$\text{ASA degradation(\%)} = \frac{[\text{SA mole}]}{[\text{ASA mole}] + [\text{SA mole}]} \times 100 \quad (28)$$

where [SA mole] and [ASA mole] are the molar concentrations of SA and ASA, respectively.

ASA degradation rate was approximated from the slope of the graph of percentage of ASA degradation against time fitted into the Leeson and Mattocks model (Eq. 29) (40).

$$\log \frac{[A_0] \left([D_0]^{1/2} + [C]^{1/2} \right)^2}{[A] \left([D_0]^{1/2} + [C_0]^{1/2} \right)^2} = \frac{[D_0]^{1/2} k_p^{3n/2} t}{2.303} \quad (29)$$

where $[A_0]$ and $[C_0]$ are the initial ASA and SA concentrations, respectively. $[A]$ and $[C]$ indicate concentrations of ASA and SA at time t , respectively. $[D_0]$ is the total concentration of ASA and SA. p refers to the vapor pressure. k is obtained from the slope of Leeson and Mattocks model and is related the rate constant. n is the order of sorption reaction with respect to p .

ASA Content Uniformity

ASA content in ten randomly chosen tablets was determined using the HPLC method described in the previous section.

Data Analysis

All graphs were plotted using the software (GraphPad Prism, v.6.01, USA). The same software was used to perform linear regression. Data fitting to the GAB model, Young and Nelson model, and Leeson and Mattocks model was carried out using Matlab (R2013b, MathWorks, USA).

RESULTS

Morphology, Size, and Size Distribution

SEM images of the starch grains (Fig. 1) showed that there were no obvious differences in the morphology of high-amylose starch and high-amylopectin starch. The starch grains can be described as having irregular and angular surfaces with polygonal shapes. However, results from the size characterization (Table I) revealed that high-amylopectin starch had slightly larger grain size with wider size distribution compared to high-amylose starch.

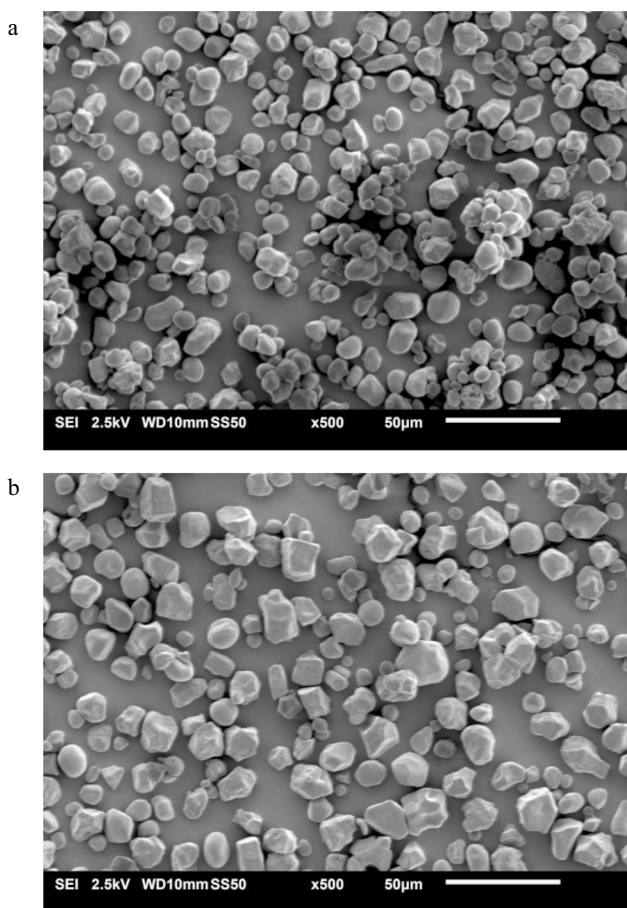


Fig. 1 Representative SEM images of **a** high-amylose starch and **b** high-amylopectin starch

XRD Pattern

XRD patterns of the two starches are shown in Fig. 2 and the diffractograms are generally in agreement with those from other studies (41, 42). No obvious changes in XRD patterns of the starches after storage at different RH conditions were detected. Distinct peaks at 2θ values of about 15° (peak 1), 18° (peak 2), and 24° (peak 3) were observed in the XRD patterns of high-amylopectin starch. In contrast, high-amylose starch showed peaks at 2θ values of around 17° (peak 1) and 20° (peak 2). The high-amylopectin starch generally exhibited higher relative crystallinity than high-amylose starch, except samples equilibrated at 75% RH

Table I Characteristics of High-Amylose Starch and High-Amylopectin Starch

Starch type	Size (µm)			Span	Relative crystallinity (%)		
	D ₁₀	D ₅₀	D ₉₀		33% RH	53% RH	75% RH
High amylose	5.90	8.80	12.0	0.69	37.9 ± 0.29	38.9 ± 0.30	40.4 ± 0.75
High amylopectin	6.83	11.2	16.2	0.83	40.2 ± 1.03	41.2 ± 0.61	40.1 ± 0.65

± represents standard deviation

where both starches had almost comparable relative crystallinity (Table I). Additionally, the relative crystallinity of high-amylose starch was close to that of high-amylopectin starch when both starches were equilibrated at 75% RH.

Interaction of Moisture With Starch

Moisture Content

Figure 3 shows that after oven drying, both starches had comparable moisture content. Differences in the moisture content manifested after storage at different RH whereby high-amylose starch had higher moisture content than high-amylopectin starch at all RH conditions. For both starches, the moisture content showed increasing trend with increasing storage RH.

Moisture Sorption-Desorption Isotherm

Moisture sorption-desorption isotherms of the starches are shown in Fig. 4a. The general shape of the isotherms is similar for both starches. The isotherms showed non-linear increment in moisture content with increasing water activity and had the characteristic sigmoidal shape curve, similar to typical moisture sorption-desorption isotherm of starch (26, 43). Hysteresis between sorption and desorption isotherms was also observed over the entire range of water activity studied. The area of hysteresis was larger for high-amylose starch than for high-amylopectin starch. The areas of hysteresis were approximately 1.87 and 1.12 a_w% moisture for high-amylose starch and high-amylopectin starch, respectively.

GAB Modeling

Table II shows results of fitting the moisture sorption-desorption data to the GAB model. The experimental data were relatively well fitted to the GAB model (R² = 1). While high-amylose starch had similar isotherm in shape as high-amylopectin starch (Fig. 4a), values of the parameters obtained from the GAB model were dissimilar between the starches. This suggests that the starches have their definitive modes of interaction with moisture. Values of M_m and C_{GAB} derived from the sorption isotherm were lower than the values obtained from the desorption isotherm. In contrast, K_{GAB} values from the sorption isotherm were slightly higher than

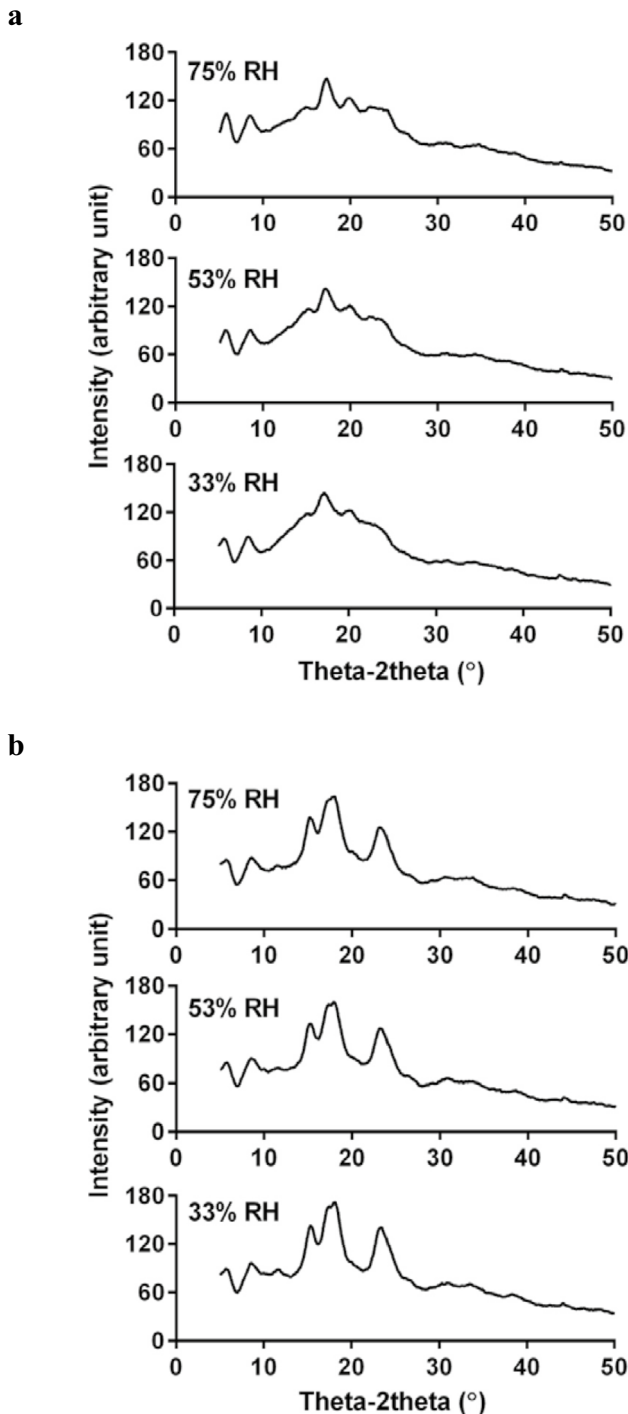


Fig. 2 XRD patterns of **a** high-amylose starch and **b** high-amylopectin starch

K_{GAB} values obtained from the desorption isotherm. C_{GAB} , a constant that is related to total heat of the first layer of sorption, was observed to have higher magnitude compared to K_{GAB} . This confirmed the stronger interaction between sorption sites on the starch matrix and water molecules of the monolayer moisture. The lower magnitude of K_{GAB} , a

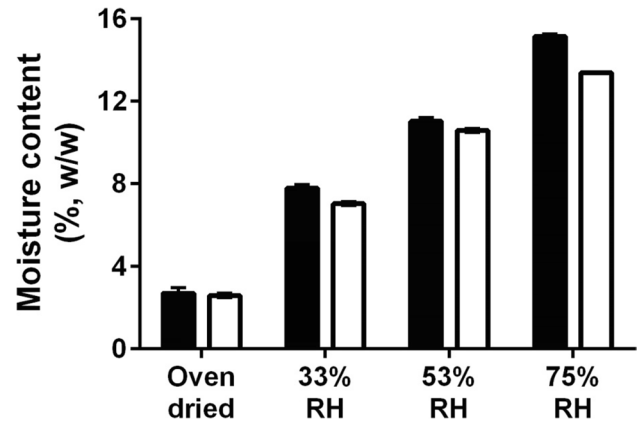


Fig. 3 Moisture content of high-amylose starch (*black square*) and high-amylopectin starch (*white square*) after subjected to different storage conditions

constant that is related to heat of multilayer sorption, implied weaker interaction of water molecules in the bulk or multilayer moisture compared to the monolayer moisture.

In general, high-amylose starch had higher M_m than high-amylopectin starch. Accordingly, SSA approximated from M_m was also higher for high-amylose starch than for high-amylopectin starch. The SSA values approximated from M_m of the corresponding sorption isotherm were 296.87 and 253.26 m^2/g for high-amylose and high-amylopectin starches, respectively. Similarly, the SSA values obtained using M_m from the corresponding desorption isotherm were about 430.38 and 319.70 m^2/g for high-amylose starch and high-amylopectin starch, respectively. In terms of the energy parameters, high-amylose starch was found to have higher C_{GAB} than high-amylopectin starch for the parameters derived from the sorption and desorption isotherms. This indicates higher driving force for moisture sorption in high-amylose starch, specifically for formation of monolayer moisture. K_{GAB} values derived from the sorption isotherm were almost comparable for the two starches, whereas the K_{GAB} derived from the desorption isotherm was marginally higher for high-amylopectin starch than for high-amylose starch.

Locality of Sorbed Moisture

The experimental data were found to fit well to the Young and Nelson model ($R^2 > 0.90$) (Table III). Percentage of the total moisture content distributed into monolayer moisture, externally adsorbed moisture, and internally absorbed moisture is shown in Fig. 4b. Initially, most of the sorbed moisture was found as monolayer moisture and the percentage reduced gradually as water activity increased. With increasing water activity, fraction of the sorbed moisture distributed as externally adsorbed moisture and internally

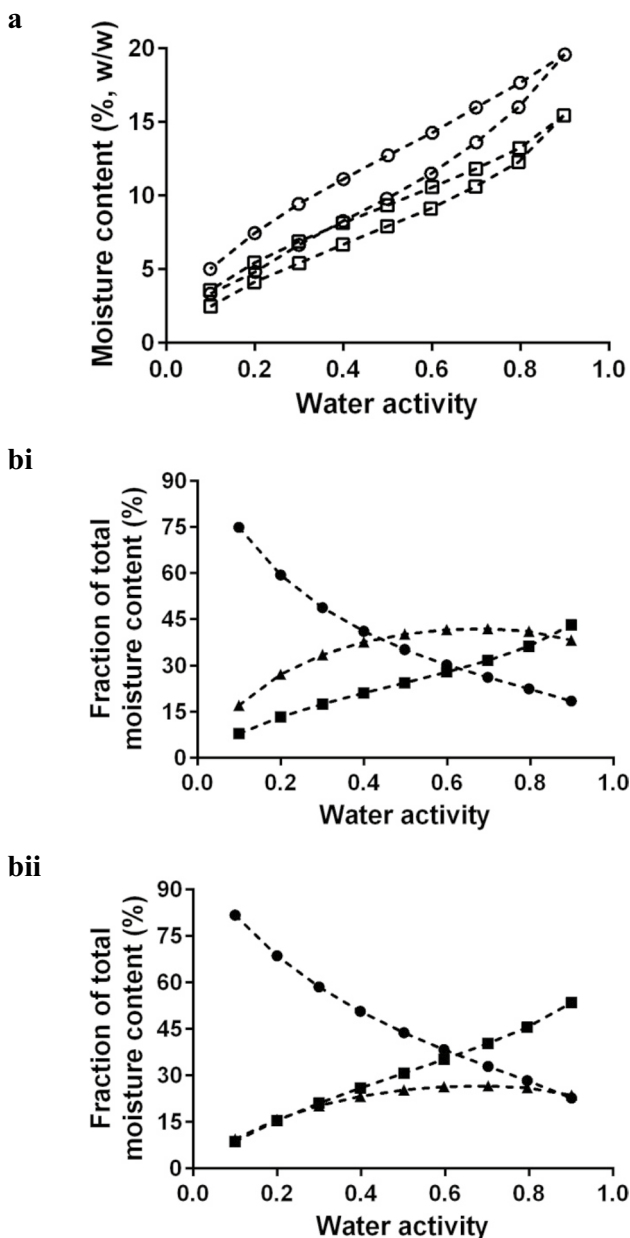


Fig. 4 Moisture interaction of starches having different amylose-amylopectin ratio. **a** Moisture sorption-desorption isotherm of high-amylose starch (white circle) and high-amylopectin starch (white square). **b** Locality of sorbed moisture as monolayer moisture (black circle), externally adsorbed moisture (black square), and internally absorbed moisture (black triangle), expressed as fraction of the total moisture content in (i) high-amylose starch and (ii) high-amylopectin starch

absorbed moisture increased whereby externally adsorbed moisture showing an almost linear increase, while internally absorbed moisture exhibited gradual increment towards a plateau level.

For high-amylose starch, at water activity >0.4, considerable proportion of the sorbed moisture existed as internally absorbed moisture. In contrast, proportion of the sorbed

Table II Fitting Coefficients for GAB Model

a GAB parameters from sorption isotherm		
GAB parameters	Starch type	
	High-amylose starch	High-amylopectin starch
M_m (g/100 g)	8.37 (7.95, 8.80)	7.14 (6.31, 7.80)
C_{GAB}	8.79 (7.68, 9.91)	6.56 (4.93, 8.22)
K_{GAB}	0.68 (0.66, 0.70)	0.69 (0.64, 0.73)
<i>Goodness of fit</i>		
SSE	0.07	0.18
R^2	1.00	1.00
$R^2_{adjusted}$	1.00	1.00
RMSE	0.11	0.18
b GAB parameters from desorption isotherm		
GAB parameters	Starch type	
	High-amylose starch	High-amylopectin starch
M_m (g/100 g)	12.1 (11.2, 13.1)	9.02 (8.16, 9.88)
C_{GAB}	15.8 (11.9, 15.7)	10.3 (8.42, 12.2)
K_{GAB}	0.49 (0.45, 0.54)	0.57 (0.52, 0.61)
<i>Goodness of fit</i>		
SSE	0.16	0.15
R^2	1.00	1.00
$R^2_{adjusted}$	1.00	1.00
RMSE	0.16	0.16

Numbers in parentheses represent the upper and lower bounds of the 95% confidence interval

SSE sum of squares, RMSE root-mean-square error

Table III Fitting Coefficients for Young and Nelson Model

Young and Nelson parameters	Starch type	
	High-amylose starch	High-amylopectin starch
A_{Y-N}	0.04 (0.03, 0.04)	0.03 (0.02, 0.04)
B_{Y-N}	0.09 (0.07, 0.10)	0.03 (0.01, 0.06)
E	0.02	0.02
<i>Goodness of fit</i>		
SSE	0.00	0.00
R^2	1.00	0.99
$R^2_{adjusted}$	1.00	0.99
RMSE	0.00	0.00

Numbers in parentheses represent the upper and lower bounds of the 95% confidence interval

SSE sum of squares, RMSE root-mean-square error

moisture found as internally absorbed moisture in high-amylopectin starch was low and at water activity >0.6, bulk of the moisture taken up by high-amylopectin starch was located externally. From Fig. 4b, it was also observed that at water activity >0.6, moisture distributed into externally adsorbed moisture was greater than that of monolayer moisture for both high-amylose and high-amylopectin starches. Therefore, allowing for estimation of extent of multilayer

moisture. The results are presented in Table IV. The multilayer moisture increased as water activity increased and high-amylose starch had slightly higher multilayer moisture than high-amylopectin starch.

Tabletability, Compactibility, and Compressibility

Tableting properties of the starches are summarized in Table V. Tabletability and compactibility of high-amylose starch were more sensitive to the effect of RH as seen from the marked reduction in the tabletability index, *b* value, and σ_0 of high-amylose starch equilibrated to 75% RH. At RH of 33 and 53%, high-amylose starch had higher tabletability index than high-amylopectin starch. However, at 75% RH, high-amylopectin starch was found to have higher tabletability index than high-amylose starch. A material with higher tabletability index suggests that it is more sensitive to change in the compression pressure,

which translated to the production of higher tensile strength tablets at a lower compression pressure.

The constant *b* value of Ryshkewitch-Duckworth equation is related to pore distribution within a tablet (44). A higher *b* value indicates faster increase in the tablet tensile strength as the porosity is reduced. Overall, high-amylose starch and high-amylopectin starch had comparable *b* values at 33 and 53% RH. However, at 75% RH, high-amylopectin starch had a considerably higher *b* value than that for high-amylose starch. Another parameter of the Ryshkewitch-Duckworth equation, σ_0 , was found to be greater for high-amylose starch at 33 and 53% RH. However, high-amylopectin starch that had been equilibrated to 75% RH had higher σ_0 than high-amylose starch equilibrated to the same condition. The 53 and 75% RH equilibrated high-amylopectin starch samples had comparable σ_0 .

From the Heckel parameters, high-amylose starch showed a lower yield pressure than high-amylopectin starch. For both starches, the yield pressure decreased with increasing

Table IV Distribution of Sorbed Moisture in High-Amylose Starch and High-Amylopectin Starch at Water Activity >0.6 as Estimated From Young and Nelson Model

a High-amylose starch					
Water activity	Moisture content (% w/w)	$A_{Y-N} \theta_{Y-N}$ (% w/w)	$A_{Y-N} (\theta_{Y-N} + \alpha)$ (% w/w)	$B_{Y-N} \Phi$ (% w/w)	Multilayer moisture (% w/w)
0.7	14.2	3.72 (26.3)	4.50 (31.8)	5.94 (42.0)	0.78 (5.51)
0.8	16.6	3.73 (22.5)	6.01 (36.3)	6.81 (41.1)	2.28 (13.8)
0.9	20.1	3.74 (18.6)	8.68 (43.1)	7.70 (38.3)	4.94 (24.5)
b High amylopectin starch					
Water activity	Moisture content (% w/w)	$A_{Y-N} \theta_{Y-N}$ (% w/w)	$A_{Y-N} (\theta_{Y-N} + \alpha)$ (% w/w)	$B_{Y-N} \Phi$ (% w/w)	Multilayer moisture (% w/w)
0.7	8.62	2.84 (33.0)	3.48 (40.4)	2.30 (26.7)	0.64 (7.41)
0.8	10.0	2.85 (28.4)	4.58 (45.6)	2.61 (26.0)	1.73 (17.2)
0.9	12.5	2.86 (22.8)	6.71 (53.5)	2.96 (23.7)	3.85 (30.7)

Numbers in parentheses represent moisture associated with the different locations as a percentage of the total moisture content $A_{Y-N} \theta_{Y-N}$ monolayer moisture, $A_{Y-N} (\theta_{Y-N} + \alpha)$ externally adsorbed moisture, $B_{Y-N} \Phi$ internally absorbed moisture

Table V Tableting Properties of High-Amylose Starch and High-Amylopectin Starch After Storage at Different RH

a High-amylose starch							
RH (%)	Tabletability index	Ryshkewitch-Duckworth parameters		Heckel parameters			
		<i>b</i>	σ_0 (MPa)	Yield pressure (MPa)	D_0	D_a	D_b
33	$5.84 \times 10^{-3} \pm 0.00$	10.7 ± 0.38	9.94 ± 0.92	62.0 ± 0.06	0.43 ± 0.01	0.48 ± 0.00	0.05 ± 0.01
53	$7.72 \times 10^{-3} \pm 0.00$	9.27 ± 0.90	10.5 ± 1.63	45.2 ± 0.55	0.41 ± 0.00	0.44 ± 0.00	0.03 ± 0.01
75	$3.80 \times 10^{-3} \pm 0.00$	4.39 ± 1.09	3.28 ± 0.67	34.4 ± 0.55	0.39 ± 0.01	0.45 ± 0.01	0.06 ± 0.01
b High-amylopectin starch							
RH (%)	Tabletability index	Ryshkewitch-Duckworth parameters		Heckel parameters			
		<i>b</i>	σ_0 (MPa)	Yield pressure (MPa)	D_0	D_a	D_b
33	$3.72 \times 10^{-3} \pm 0.00$	10.6 ± 0.79	7.75 ± 1.25	73.3 ± 0.17	0.43 ± 0.00	0.47 ± 0.01	0.03 ± 0.00
53	$5.20 \times 10^{-3} \pm 0.00$	9.75 ± 0.35	9.38 ± 0.74	53.4 ± 1.68	0.41 ± 0.01	0.43 ± 0.00	0.03 ± 0.01
75	$4.93 \times 10^{-3} \pm 0.00$	8.93 ± 0.81	9.53 ± 1.93	41.6 ± 3.04	0.39 ± 0.01	0.45 ± 0.01	0.06 ± 0.02

± represents standard deviation

RH. A lower yield pressure means that the material is more deformable under pressure. Despite their differences in yield pressure values, both starches showed rather similar die filling properties as evidenced from the comparable D_0 , D_a , and D_b values. For both starches, D_a was slightly larger than D_0 . This could be ascribed to the elastic deforming property of starch. As such, unlike materials that undergo considerable plastic deformation or brittle fragmentation, there is less particle rearrangement when compressed. As RH increased, D_0 and D_a values decreased, indicating reduced efficiency of the particles to pack in the die.

Viscoelastic Recovery

The powder expansion behavior during decompression was assessed as viscoelastic recovery. In general, the change in tablet dimensions showed an increasing trend as RH increased (Fig. 5). It was found that overall, tablets produced from high-amylopectin starch had greater change in tablet dimensions than high-amylose starch tablets. ASA tablets formulated with the different types of starch also exhibited similar trend (Fig. 6). The effect of applied compression pressure varied with the types of starch and equilibrium RH. For tablets produced from 33% RH equilibrated starches, the change in the tablet dimensions initially increased, reached the maximum at 127 MPa, and then decreased. Similar trend was observed for tablets produced from 53% RH equilibrated starches. The change in tablet dimensions with compression pressure was less remarkable for 75% RH equilibrated starches.

Properties of ASA Tablets

ASA content uniformity in the tablets was found to be good. The respective ASA content for the different formulations was $98.50\% \pm 1.33\%$, $99.51\% \pm 0.75\%$, and $99.50\% \pm 1.46\%$ for tablets prepared from high-amylose starch, 1:1 mixture of high-amylose and high-amylopectin starches, and high-amylopectin starch. Therefore, influence of drug content variation on ASA degradation was negligible. Percentage of ASA degradation in tablets produced from the starches of different amylose-amylopectin ratio is presented in Fig. 7. Differences in the percentage degradation of ASA among the tablets were not large but significant. Clearly, ASA degradation was impacted by the amylose-amylopectin ratio. Percentage of ASA degradation in tablets formulated with high-amylose starch was found to be consistently lower compared to that in the high-amylopectin starch tablets. Percentage of ASA degradation in tablets containing 1:1 mixture of high-amylose and high amylopectin starches was intermediate to the tablets containing only the high-amylose starch or high-amylopectin starch. After 90 days of storage, ASA degradation in tablets produced from high-amylopectin

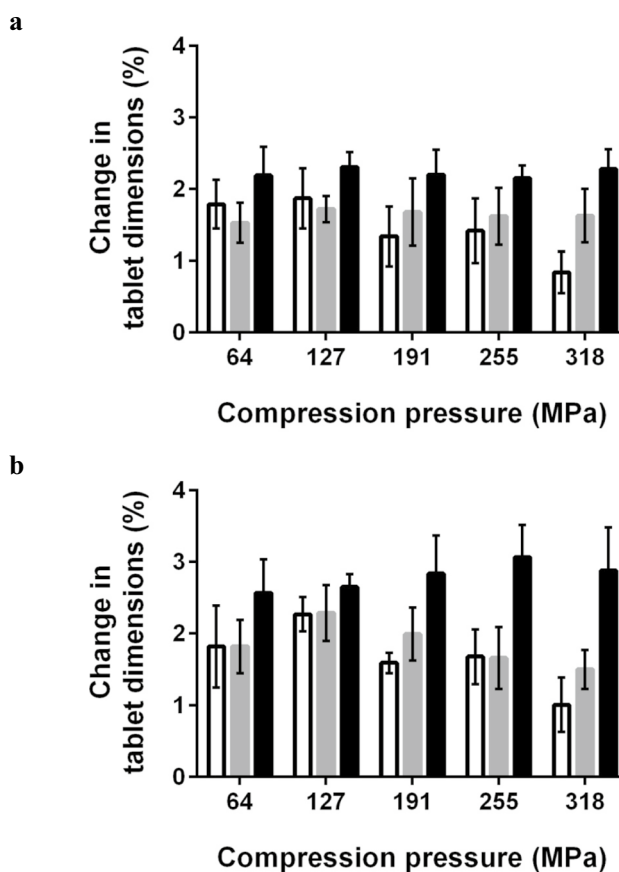


Fig. 5 Percentage change in dimensions of tablets produced from **a** high-amylose starch tablets and **b** high-amylopectin starch tablets starch equilibrated to different conditions — 33% RH (white square), 53% RH (gray square), and 75% RH (black square)

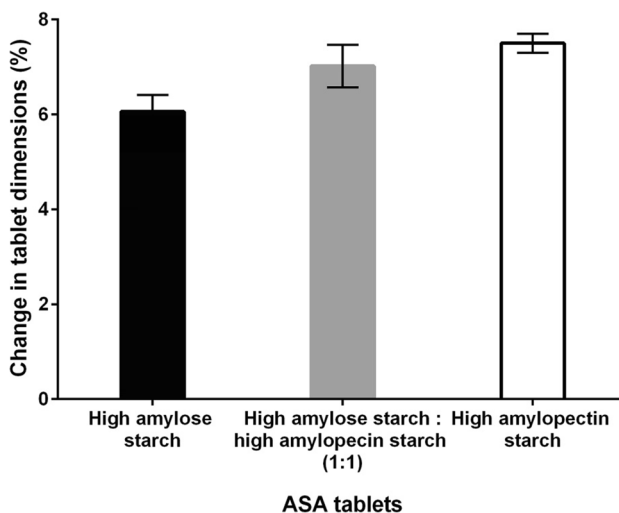


Fig. 6 Change in dimensions of ASA tablets produced from high-amylose starch (black square), 1:1 mixture of high-amylose and high-amylopectin starches in 1:1 ratio (gray square), and high-amylopectin starch (white square), post 24 h storage at 75% RH, 40°C

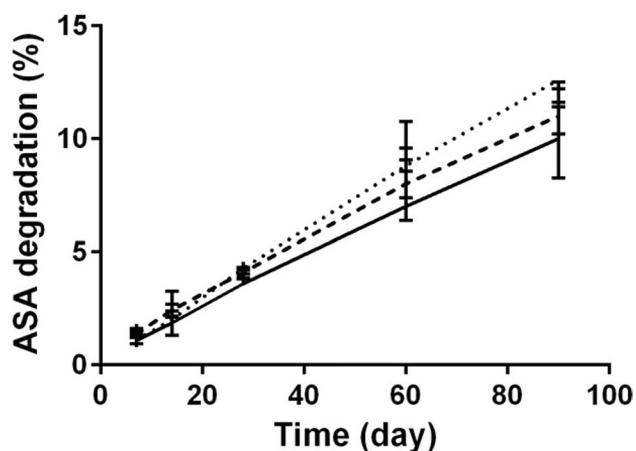


Fig. 7 Percentage of ASA degradation in tablets produced from high-amylose starch (*solid line*), 1:1 mixture of high-amylose and high-amylopectin starches (*dashed line*), and high-amylopectin starch (*dotted line*) after storage at 75% RH, 40°C

starch was 16.96% and 9.62% greater than the degradation in tablets containing high-amylose starch, and tablets containing 1:1 mixture of high-amylose and high-amylopectin starches, respectively.

Fitting of the degradation data to the Leeson and Mattocks model was successful with $R^2 > 0.90$. Rate of ASA degradation was approximated from the slope of Leeson and Mattocks model and found to be 1.94×10^{-3} , 1.98×10^{-3} , and $2.20 \times 10^{-3} \% \cdot \text{day}^{-1}$ for tablets containing high-amylose starch, 1:1 mixture of high-amylose and high-amylopectin starches, and high-amylopectin starch, respectively.

DISCUSSION

Moisture Interaction of Starches With Different Amylose-Amylopectin Ratio

Starch is made up of predominantly two polysaccharides: linear chain amylose and highly branched amylopectin. The organization of amylose and amylopectin in starch gives starch its semi-crystalline structure (23). Amylose-amylopectin ratio of starch has been found to vary between and within botanical species (45) with implications on the molecular packing of the starch grains, whereby starches of higher amylopectin ratio have been reported to have higher relative crystallinity (25, 46, 47).

Interaction of moisture with starch is due to hydrogen bonding of water molecules to the hydroxyl groups on the polysaccharides (48). Although hysteresis could be observed in the isotherms of high-amylose starch and high-amylopectin starch, the areas of hysteresis loop were not

comparable (Fig. 4a). This could be attributed to differences in the polymeric structural organization, hence affecting accessibility and holding capacity of water molecule binding sites. Molecular packing or arrangement in solids is known to influence the interaction of the materials with water molecules (19, 20). Crystallinity in amylopectin regions of starch results from intertwining of the outer chains of amylopectin in the form of double helices forming ordered regions that appear as “crystalline lamellae” (49). While amylose is also capable of forming double helices, packing of the double helices is less compact than those of amylopectin (49, 50). Consequently, the hydroxyl groups in amylopectin are more constrained and become less accessible to interact with the ubiquitous water molecules as vapor in the environment. Differences in moisture interaction due to different packing arrangements in amylose and amylopectin could be observed from the results of the GAB as well as Young and Nelson model fittings.

Compared to high-amylopectin starch, high-amylose starch had higher M_m for both sorption and desorption isotherms. Correspondingly, high-amylose starch also had higher SSA than high-amylopectin starch. Although the monolayer moisture values obtained from fitting sorption data into the Young and Nelson model was not directly comparable with the values obtained from the GAB model, the same trend was observed in which high-amylose starch had higher monolayer moisture content than high-amylopectin starch for the range of water activity evaluated. The monolayer moisture content obtained from the Young and Nelson model ranged from 3.17 to 3.74% and 2.43 to 2.86% for high-amylose starch and high-amylopectin starch, respectively. The lower relative crystallinity of high-amylose starch could also contribute to the greater proportion of sorbed moisture found as internally absorbed moisture. This is due to sorption of moisture occurring not only on the surfaces but also in the bulk structure of solids with lower relative crystallinity.

Amylose-Amylopectin Ratio of Starch and Tableting Properties

Presence of moisture is known to affect tableting properties as moisture often plays an important role in rearrangement, packing, and bond formation of the particles during tableting. Tabletability indices of the starches showed optima around the 53% RH equilibrated starch samples. The initial increase in tabletability index with RH could be attributed to the ability of moisture to act as a lubricant, hence facilitating volume reduction. This causes greater degree of powder bed densification and particle consolidation during compression (51). The improved densification in the presence of moisture was also observed as reduction in the yield pressure, as has been reported in other studies (52, 53). With increasing

compression pressure, tablet density approaches true density of the material and the tablet porosity reaches lower porosity at a faster rate. Tablets of lower porosity generally have larger areas of interparticulate bonding, therefore forming stronger tablets. This was also supported by the highest σ_0 observed for tablets produced from the starch samples equilibrated to 53% RH. Another possible explanation for the improvement in tablet tensile strength as RH increased from 33 to 53% could be due to moisture facilitated stronger interparticulate bonding by hydrogen bonding. Furthermore, moisture could smoothen micro-irregularities and facilitate proximal contacts between surfaces, therefore, reducing the interparticulate distances and increasing the van der Waals forces (54, 55).

However, excessive amount of moisture was detrimental to the tablet tensile strength as seen from the reduced tableability index, b value, and σ_0 of the starch samples equilibrated to 75% RH despite the lowered yield pressure. The subsequent reduction in tablet tensile strength occurring at higher RH has also been reported in other studies (56–58). It has been suggested that balance between the amount of monolayer moisture, externally adsorbed moisture, and internally absorbed moisture influences tablet tensile strength (1). From Fig. 4b, at water activity >0.6 , the fraction of sorbed moisture distributed as externally adsorbed moisture was greater than the monolayer moisture. As such, for the starch samples stored at 75% RH, it could be implied that the amount of externally adsorbed moisture was higher. Thus, the reduced tablet tensile strength at high RH could be attributed to conditions where the labile surface moisture present could reduce or disrupt the interparticulate bonding. This was supported by the b value being the lowest for the starches equilibrated to 75% RH (Table V). The lower b value suggests that tablet tensile strength does not increase as much despite the reduction in tablet porosity. This also explains the reduced tableability index and σ_0 observed for 75% RH equilibrated starch samples, albeit a more prominent reduction was observed in tablets produced from high-amylose starch.

With reference to the amylose-amylopectin ratio and tableting properties, tablets produced from high-amylose starch were more susceptible to reduction in tablet tensile strength when stored under high RH. An analysis of locality of the sorbed moisture revealed that at high RH, amount of moisture adsorbed on the surface in excess to the monolayer moisture (extent of multilayer moisture) was higher in high-amylose starch (Table IV). The excess monolayer moisture could disrupt the interparticulate bonding, consequently lowering tablet tensile strength. Reduced tablet tensile strength when moisture level exceeded monolayer moisture has also been demonstrated in microcrystalline cellulose tablets (58).

Viscoelastic recovery of the tablets was also investigated as change in tablet dimensions in relation to the storage RH and the types of starch. Generally, the change in tablet dimensions increased as RH increased. This could indirectly contribute to the reduced tablet tensile strength as the RH increased from 53 to 75%, in addition to the moisture layer that interfered with interparticle bonds. Excessive viscoelastic recovery during decompression could disrupt the interparticle bonds formed during the compression phase, hence compromising tablet tensile strength. It was also observed that the viscoelastic recovery varied with the compression pressure and the types of starch. Several studies have reported that viscoelastic recovery can increase, decrease, or remain unaffected with the change in compression pressure (59, 60). For starches equilibrated to 53% RH or lower, when compared to tablets equilibrated at 75% RH, the viscoelastic recovery decreased with increasing compression pressure, particularly when the compression pressure exceeded 127 MPa (Fig. 5). This could be because the high pressure brought the particles closer together, creating intensive particle-particle forces that hindered the expansion during the relaxation phase (59). The moisture layer on starches equilibrated to 75% RH could have weakened the compression pressure-viscoelastic recovery relationship that was observed in starches equilibrated to lower RH by acting as a cushion to the applied force. Therefore, while viscoelastic recovery could be observed in both starches, the extent varied with the types of starch, compression pressure used and environmental RH.

Amylose-Amylopectin Ratio of Starch and ASA Stability

Stability of a moisture-sensitive drug in formulations is affected by not only the amount of moisture present but also how it is retained in the formulations. Differences in the percentage of ASA degradation observed between tablets produced with high-amylose starch and high-amylopectin starch suggested that moisture retention in starch was affected by the ratio of amylose to amylopectin. This finding was supported by the lowered ASA degradation in tablets with high-amylose starch while ASA degraded faster when high amylopectin was used instead. For ASA tablets containing a 1:1 mixture of high-amylose and high-amylopectin starches, the ASA degradation was intermediate, suggesting a linearly proportionated outcome. Viscoelastic recovery could change tablet porosity, which could affect moisture exposure of ASA within the tablet matrix. Tablet porosity is often purported as the factor related to the ease of tablet components to come into contact with moisture/water, particularly in tablet disintegration and dissolution. However, in tablets formulated with elastically deforming materials, it has been reported that tablet porosity exerts minimal influence on drug degradation

(61). Furthermore, accumulation of SA produced from ASA degradation can affect tablet pore volume and size with prolonged storage, consequently confounding the correlation between ASA stability and pore size (62). Therefore, the stability could mainly be related to the moisture interaction of the formulation components.

While high-amylose starch exhibited lower relative crystallinity than high-amylopectin starch, tablets formulated with high-amylose starch resulted in better ASA stability. A study on effects microcrystalline celluloses of different crystallinity on the stability of moisture-sensitive drugs also reported better drug stability in formulations containing microcrystalline of lower crystallinity (9, 63). Clearly, molecular packing as reflected by crystallinity influences their interaction with moisture.

Hydrolysis of a moisture-sensitive drug in solid dosage form typically occurs when the drug dissolves in the sorbed moisture layer (40). Exposure of tablets to a fixed RH environment allows the sorbed moisture within the constituents to reach equilibrium state. This condition is akin to the process for obtaining moisture sorption-desorption isotherm, in which the sample is equilibrated to a particular RH before moving to the next RH condition. As such, results from fitting of the isotherm data to the GAB model as well as the Young and Nelson model could be extended to explain the reactivity of the sorbed moisture in relation to the amylose-amylopectin ratio of the starches.

An inverse relationship between the GAB parameters (M_m and C_{GAB}) and percentage of ASA degradation was observed. M_m is related to the number of water molecule binding sites. As high-amylose starch was found to have higher M_m than high-amylopectin starch, the lower percentage of ASA degradation in high-amylose starch tablets could be attributed to the greater number of water molecule binding sites of high-amylose starch. C_{GAB} is related to the total heat of monolayer moisture; the higher C_{GAB} value of high-amylose starch implied greater extent of interaction of moisture with the starch at monolayer moisture level. Therefore, the moisture may not easily be detached and be available for reaction in ASA degradation. Because the difference in K_{GAB} between the two starches was marginal, K_{GAB} may not be able to provide a clear distinction between high-amylose starch and high-amylopectin starch regarding the reactivity of sorbed moisture. Accordingly, K_{GAB} , a constant that is related to binding of multilayer moisture on monolayer moisture formed on surface of the substrate, could be less descriptive for reactivity of sorbed moisture.

The lower ASA degradation in high-amylose starch tablets could also be attributed to the locality of the sorbed moisture. Indeed, importance of locality of sorbed moisture on functionality of excipients has been illustrated in crospovidone as a tablet disintegrant (64). In this study, findings from distribution of sorbed moisture were used to facilitate understanding

of reactivity of sorbed moisture in relation to drug hydrolysis. In high-amylose starch, it was observed that at water activity >0.4 , most of the sorbed moisture was the internally absorbed moisture. As such, the sorbed moisture was less available for hydrolytic reaction. In contrast, the locality of internally absorbed moisture in high-amylopectin starch was consistently lower than that of high-amylose starch throughout the range of water activity studied and at water activity >0.6 , most of the sorbed moisture was associated with externally adsorbed moisture (Table IV). Therefore, as the tablets were stored at 75% RH, the higher amount of externally located moisture in high-amylopectin starch had been the causative factor to greater ASA degradation. Interestingly, while tableting properties of high-amylose starch were more at risk of reduced tableting and compactibility at high RH (Table V), tablets with high-amylose starch had better stability profile than that of high-amylopectin starch. This may suggest that the larger values of M_m and C_{GAB} of high-amylose starch, and distribution of moisture into internally absorbed moisture are more instrumental in stability of hydrolysable drugs than tableting properties.

CONCLUSIONS

This study elucidated differences in tableting properties and moisture interactivities related to the amylose-amylopectin ratio of starch. Tableting properties of the starches were found to be affected not only by environmental RH but also by relative locality of the sorbed moisture. High-amylose starch demonstrated better tableting than high-amylopectin starch at 33 and 53% RH. However, at 75% RH, high-amylopectin starch exhibited better tableting than high-amylose starch but drug stability was poorly compromised. At high RH, high-amylose starch was observed to have larger amount of moisture adsorb on the surface in excess to the monolayer moisture which disrupted bonding between the particles when compacted. This study also demonstrated that availability of binding sites for the water molecules, strength of moisture-starch interaction, and locality of sorbed moisture were determinant on the susceptibility of moisture-sensitive drugs present to degrade.

While this study has shown that variations in amylose-amylopectin ratio of starch could influence the effects of moisture on tableting properties and degradation of moisture-sensitive drugs, it should be noted that the starches used in this study were native-unmodified starches. Also, as the stability study was performed under elevated environmental RH and temperature, the results may be an exaggeration of degradation under non-stress conditions. Nonetheless, this study highlighted the importance of amylose-amylopectin ratio when changing from one type of starch to another during formulation development or product manufacture, particularly with actives that are moisture sensitive.

Acknowledgements The authors acknowledge the National University of Singapore for supporting Natalia Veronica in her doctorate studies as a recipient of the National University of Singapore Graduate Research Scholarship.

Author Contribution Natalia Veronica: conceptualization, data curation and analysis, investigation, methodology, preparing original draft. Celine Valeria Liew: conceptualization, supervision, review and edit manuscript. Paul Wan Sia Heng: conceptualization, supervision, review and edit manuscript.

Funding Open Access funding enabled and organized by CAUL and its Member Institutions Funding for the research work is provided by GEANUS PPR L (N-148-000-008-001).

Declarations

Conflict of Interest The authors declare no competing interests.

Open Access This article is licensed under a Creative Commons Attribution 4.0 International License, which permits use, sharing, adaptation, distribution and reproduction in any medium or format, as long as you give appropriate credit to the original author(s) and the source, provide a link to the Creative Commons licence, and indicate if changes were made. The images or other third party material in this article are included in the article's Creative Commons licence, unless indicated otherwise in a credit line to the material. If material is not included in the article's Creative Commons licence and your intended use is not permitted by statutory regulation or exceeds the permitted use, you will need to obtain permission directly from the copyright holder. To view a copy of this licence, visit <http://creativecommons.org/licenses/by/4.0/>.

References

- Nokhodchi A, Ford JL, Rubinstein MH. Studies on the interaction between water and hydroxypropyl methylcellulose. *J Pharm Sci*. 1997;86(5):608–15. <https://doi.org/10.1021/js960279a>.
- Quodbach J, Kleinebudde P. Performance of tablet disintegrants: impact of storage conditions and relative tablet density. *Pharm Dev Technol*. 2015;20(6):762–8. <https://doi.org/10.3109/10837450.2014.920357>.
- Rohrs BR, Thamann TJ, Gao P, Stelzer DJ, Bergren MS, Chao RS. Tablet dissolution affected by a moisture mediated solid-state interaction between drug and disintegrant. *Pharm Res*. 1999;16(12):1850–6.
- Sandler N, Reiche K, Heinamaki J, Yliruusi J. Effect of moisture on powder flow properties of theophylline. *Pharmaceutics*. 2010;2(3):275–90. <https://doi.org/10.3390/pharmaceutics2030275>.
- Viljoen JM, Steenekamp JH, Marais AF, Kotze AF. Effect of moisture content, temperature and exposure time on the physical stability of chitosan powder and tablets. *Drug Dev Ind Pharm*. 2014;40(6):730–42. <https://doi.org/10.3109/03639045.2013.782501>.
- Zong Z, Desai SD, Kaushal AM, Barich DH, Huang HS, Munson EJ, et al. The stabilizing effect of moisture on the solid-state degradation of gabapentin. *AAPS PharmSciTech*. 2011;12(3):924–31. <https://doi.org/10.1208/s12249-011-9652-8>.
- Awa K, Shinzawa H, Ozaki Y. The effect of microcrystalline cellulose crystallinity on the hydrophilic property of tablets and the hydrolysis of acetylsalicylic acid as active pharmaceutical ingredient inside tablets. *AAPS PharmSciTech*. 2015;16(4):865–70. <https://doi.org/10.1208/s12249-014-0276-7>.
- Du J, Hoag SW. The influence of excipients on the stability of the moisture sensitive drugs aspirin and niacinamide: comparison of tablets containing lactose monohydrate with tablets containing anhydrous lactose. *Pharm Dev Technol*. 2001;6(2):159–66. <https://doi.org/10.1081/pdt-100000742>.
- Hockerfelt MH, Alderborn G. The crystallinity of cellulose controls the physical distribution of sorbed water and the capacity to present water for chemical degradation of a solid drug. *Int J Pharm*. 2014;477(1–2):326–33. <https://doi.org/10.1016/j.ijpharm.2014.10.034>.
- The United States Pharmacopeia. Water-solid interactions in pharmaceutical systems. USP42-NF37. 42 ed. USA: Rockville: United States Pharmacopeial Convention; 2019. p. 8226-30.
- Zografi G. States of water associated with solids. *Drug Dev Ind Pharm*. 1988;14(14):1905–26. <https://doi.org/10.3109/03639048809151997>.
- Carstensen JT, Po ALW. The state of water in drug decomposition in the moist solid state: description and modelling. *Int J Pharm*. 1992;83:87–94.
- Hiew TN, Huang R, Popov I, Feldman Y, Heng PWS. A study of moisture sorption and dielectric processes of starch and sodium starch glycolate. *Pharm Res*. 2017;34(12):2675–88. <https://doi.org/10.1007/s11095-017-2252-x>.
- Young JH, Nelson GL. Research of hysteresis between sorption and desorption isotherms of wheat. *Trans Am SOC Agric Eng*. 1967;10:756–61.
- Young JH, Nelson GL. Theory of hysteresis between sorption and desorption isotherms in biological materials. *Trans Am SOC Agric Eng*. 1967;10:260–3.
- Figura LO, Teixeira AA. Water activity. *Food Physics: Physical Properties - Measurement and Applications*. 1st ed. Springer; 2007. p. 1–38.
- Agrawal AM, Manek RV, Kolling WM, Neau SH. Studies on the interaction of water with ethylcellulose: effect of polymer particle size. *AAPS PharmSciTech*. 2003;4(4):1–11.
- Saripella KK, Mallipeddi R, Neau SH. Crospovidone interactions with water. I. Calorimetric study of the effect of polyplasdone particle size on its uptake and distribution of water. *J Pharm Sci*. 2014;103(2):669–675. <https://doi.org/10.1002/jps.23846>.
- Bronlund J, Paterson T. Moisture sorption isotherms for crystalline, amorphous and predominantly crystalline lactose powders. *Int Dairy J*. 2004;14(3):247–54. [https://doi.org/10.1016/S0958-6946\(03\)00176-6](https://doi.org/10.1016/S0958-6946(03)00176-6).
- Mihiranyan A, Llagostera AP, Karmhag R, Stromme M, Ek R. Moisture sorption by cellulose powders of varying crystallinity. *Int J Pharm*. 2004;269(2):433–42. <https://doi.org/10.1016/j.ijpharm.2003.09.030>.
- Faroongsarn D, Peck GE. Thermal porosity analysis of croscarmellose sodium and sodium starch glycolate by differential scanning calorimetry. *AAPS PharmSciTech*. 2003;4(4):1–8.
- Badawy SI, Gray DB, Hussain MA. A study on the effect of wet granulation on microcrystalline cellulose particle structure and performance. *Pharm Res*. 2006;23(3):634–40. <https://doi.org/10.1007/s11095-005-9555-z>.
- Ai Y, Jane JL. Understanding starch structure and functionality. In: Sjöö M, Nilsson L, editors. *Starch in food*. 2 ed. Woodhead Publishing Series in Food Science, Technology and Nutrition. 2018:151–178. <https://doi.org/10.1016/b978-0-08-100868-3.00003-2>.
- Schirmer M, Höchstötter A, Jekle M, Arendt E, Becker T. Physicochemical and morphological characterization of different starches with variable amylose/amylopectin ratio. *Food Hydrocoll*. 2013;32(1):52–63. <https://doi.org/10.1016/j.foodhyd.2012.11.032>.
- Cheetham NWH, Tao L. Variation in crystalline type with amylose content in maize starch granules: an X-ray powder diffraction study. *Carbohydr Polym*. 1998;36:277–84.

26. Al-Muhtaseb AH, McMinn WAM, Magee TRA. Water sorption isotherms of starch powders. Part 2: Thermodynamic characteristics. *J Food Eng.* 2004;62(2):135–142. [https://doi.org/10.1016/s0260-8774\(03\)00202-4](https://doi.org/10.1016/s0260-8774(03)00202-4)
27. Rajabnezhad S, Ghafourian T, Rajabi-Siahboomi A, Missaghi S, Naderi M, Salvage JP, et al. Investigation of water vapour sorption mechanism of starch-based pharmaceutical excipients. *Carbohydr Polym.* 2020;238:116208. <https://doi.org/10.1016/j.carbpol.2020.116208>.
28. Kaur B, Ariffin F, Bhat R, Karim AA. Progress in starch modification in the last decade. *Food Hydrocoll.* 2012;26(2):398–404. <https://doi.org/10.1016/j.foodhyd.2011.02.016>.
29. Wootton M, Bamunuarachchi A. Water binding capacity of commercial produced native and modified starches. *Starch.* 1978;30(9):306–9.
30. Builders PF, Arhewoh MI. Pharmaceutical applications of native starch in conventional drug delivery. *Starch.* 2016;68(9–10):864–73. <https://doi.org/10.1002/star.201500337>.
31. Paronen P, Juslin M. Compression characteristics of four starches. *J Pharm Pharmacol.* 1983;35:627–35.
32. Adedokun MO, Itiola OA. Material properties and compaction characteristics of natural and pregelatinized forms of four starches. *Carbohydr Polym.* 2010;79(4):818–24. <https://doi.org/10.1016/j.carbpol.2009.10.009>.
33. Veronica N, Hiew TN, Liew CV, Heng PWS. Insights into the moisture scavenging properties of different types of starch in tablets containing a moisture-sensitive drug. *Mol Pharm.* 2020;17(12):4616–28. <https://doi.org/10.1021/acs.molpharmaceut.0c00804>.
34. Roquette: Safety data sheet waxy maize starch N-200. <https://www.roquette.com/food-nutrition-starch-waxy-corn> (2017). Accessed 10 Apr 2020.
35. Roquette: Safety data sheet maize starch amylo N-400. <https://www.roquette.com/food-nutrition-starch-high-amylose-corn> (2017). Accessed 10 Apr 2020.
36. Greenspan L. Humidity fixed points of binary saturated aqueous solutions. *J Res Natl Bur Stand A Phys Chem.* 1977;81(A)(1):89–96.
37. Ryshkewitch E. Compression strength of porous sintered alumina and zirconia: 9th communication to ceramography. *J Am Ceram Soc.* 1953;36(2):65–8.
38. Duckworth W. Discussion of Ryshkewitch paper. *J Am Ceram Soc.* 1953;36:68.
39. Heckel W. Density-pressure relationship in powder compaction. *Trans Metall AIME.* 1961;221:671–5.
40. Leeson LJ, Mattocks AM. Decomposition of aspirin in the solid state. *J Am Pharm Assoc.* 1958;47(5):329–33.
41. Liu H, Yu L, Simon G, Zhang X, Dean K, Chen L. Effect of annealing and pressure on microstructure of cornstarches with different amylose/amylopectin ratios. *Carbohydr Res.* 2009;344(3):350–4. <https://doi.org/10.1016/j.carres.2008.11.014>.
42. Shi YC, Capitani T, Trzasko P, Jeffcoat R. Molecular structure of a low-amylopectin starch and other high-amylose maize starches. *J Cereal Sci.* 1998;27:289–99.
43. Wang N, Brennan JG. Moisture sorption isotherm characteristics of potatoes at four temperatures. *J Food Eng.* 1991;14:269–87.
44. Roberts RJ, Rowe RC, York P. The relationship between the fracture properties, tensile strength and critical stress intensity factor of organic solids and their molecular structure. *Int J Pharm.* 1995;125:157–62.
45. Cornejo-Ramírez YI, Martínez-Cruz O, Del Toro-Sánchez CL, Wong-Corral FJ, Borboa-Flores J, Cinco-Moroyoqui FJ. The structural characteristics of starches and their functional properties. *CyTA - J Food.* 2018;16(1):1003–17. <https://doi.org/10.1080/19476337.2018.1518343>.
46. Buleón A, Colonna P, Planchot V, Ball S. Starch granules: structure and biosynthesis. *Int J Biol Macromol.* 1998;23:85–112.
47. Copeland L, Blazek J, Salman H, Tang MC. Form and functionality of starch. *Food Hydrocoll.* 2009;23(6):1527–34. <https://doi.org/10.1016/j.foodhyd.2008.09.016>.
48. Zografí G, Kontny MJ. The interaction of water with cellulose and starch derived pharmaceutical excipients. *Pharm Res.* 1986;3(4):187–94.
49. Tester RF, Karkalas J, Qi X. Starch—composition, fine structure and architecture. *J Cereal Sci.* 2004;39(2):151–65. <https://doi.org/10.1016/j.jcs.2003.12.001>.
50. Bertoft E. Understanding starch structure: recent progress. *Agronomy.* 2017;7(3):56. <https://doi.org/10.3390/agronomy7030056>.
51. Ahlneck C, Alderborn G. Moisture adsorption and tableting. I. Effect on volume reduction properties and tablet strength for some crystalline materials. *Int J Pharm.* 1989;54:131–141.
52. Nokhodchi A, Ford JL, Rowe PH, Rubinstein MH. The effect of moisture on the heckel and energy analyses of hydroxypropylmethylcellulose 2208 (HPMC K4M). *J Pharm Pharmacol.* 1996;48(11):1121–7.
53. Nokhodchi A, Rubinstein MH, Larhib H, Guyot JC. The effect of moisture content on the energies involved in the compaction of ibuprofen. *Int J Pharm.* 1995;120:13–20.
54. Malamataris S, Karidas T. Effect of particle size and sorbed moisture on the tensile strength of some tableted hydroxypropylmethylcellulose (HPMC) polymers. *Int J Pharm.* 1994;104(1):115–23.
55. Maarschalk KvV, Vromans H, Groenendijk W, Bolhuis GK, Lerk CF. Effect of water on deformation and bonding of pregelatinized starch compacts. *Eur J Pharm Biopharm.* 1997;44(3):253–60.
56. Malamataris S, Goidas P, Dimitriou A. Moisture sorption and tensile strength of some tableted direct compression excipients. *Int J Pharm.* 1991;68:51–60.
57. Malamataris S, Goidas P, Avgoustakis K. Comparative evaluation of soy polysaccharide as direct compression excipient. *Drug Dev Ind Pharm.* 1992;18(14):1575–87. <https://doi.org/10.3109/03639049209040860>.
58. Sun CC. Mechanism of moisture induced variations in true density and compaction properties of microcrystalline cellulose. *Int J Pharm.* 2008;346(1–2):93–101. <https://doi.org/10.1016/j.ijpharm.2007.06.017>.
59. Zhang J, Wu CY, Pan X, Wu C. On identification of critical material attributes for compression behaviour of pharmaceutical diluent powders. *Materials.* 2017;10(7). <https://doi.org/10.3390/ma10070845>
60. Casian T, Iurian S, Găvan A, Porfire A, Pop AL, Crişan S, et al. In-depth understanding of granule compression behavior under variable raw material and processing conditions. *Pharmaceutics.* 2022;14(1):177. <https://doi.org/10.3390/pharmaceutics14010177>.
61. Veronica N, Liew CV, Heng PWS. Insights on the role of excipients and tablet matrix porosity on aspirin stability. *Int J Pharm.* 2020;580:119218. <https://doi.org/10.1016/j.ijpharm.2020.119218>.
62. Gucluyildiz H, Banker GS, Peck GE. Determination of porosity and pore-size distribution of aspirin tablets relevant to drug stability. *J Pharm Sci.* 1977;66(3):407–14. <https://doi.org/10.1002/jps.2600660323>.
63. Mhrranyan A, Stromme M, Ek R. Influence of cellulose powder structure on moisture-induced degradation of acetylsalicylic acid. *Eur J Pharm Sci.* 2006;27(2–3):220–5. <https://doi.org/10.1016/j.ejps.2005.10.002>.
64. Hiew TN, Johan NAB, Desai PM, Chua SM, Loh ZH, Heng PWS. Effect of moisture sorption on the performance of crosppovidone. *Int J Pharm.* 2016;514(1):322–31. <https://doi.org/10.1016/j.ijpharm.2016.06.022>.

Publisher's Note Springer Nature remains neutral with regard to jurisdictional claims in published maps and institutional affiliations.